

## Article

# Coalbed Methane Enrichment Regularity and Model in the Xishanyao Formation in the Santanghu Basin, NW China

Xinning Li <sup>1</sup>, Jiamin Zhou <sup>2,\*</sup>, Lixin Jiao <sup>1</sup>, Bin Sun <sup>3</sup>, Yangyang Huang <sup>2</sup>, Diefang Huang <sup>1</sup>, Junlang Zhang <sup>1</sup> and Longyi Shao <sup>2</sup> 

<sup>1</sup> Research Institute of Exploration and Development, PetroChina Tuha Oilfield Company, Hami 839009, China; xinningli@petrochina.com.cn (X.L.)

<sup>2</sup> College of Geoscience and Surveying Engineering, China University of Mining and Technology, Beijing 100083, China; shaol@cumtb.edu.cn (L.S.)

<sup>3</sup> Department of Unconventional Resources, Research Institute of Petroleum Exploration and Development, PetroChina, Beijing 100083, China

\* Correspondence: bqt2100201010@student.cumtb.edu.cn

**Abstract:** The Santanghu Basin is a typical low-rank coal-bearing basin in northwest China, with abundant coalbed methane (CBM) resources. However, the understanding of the main controlling factors and reservoir formation models of CBM in low-rank coal is still insufficient, which has restricted the exploration and development of CBM in this region. In this paper, the CBM enrichment controlling factors and enrichment models are analyzed based on the aspects of sedimentary environment, reservoir characteristics, sealing conditions, and hydrogeological conditions after systematically analyzing the geological characteristics of coal measures. The research results indicate that the coal seams of the Xishanyao Formation in the Santanghu Basin are stably developed, with the main macerals being vitrinite and a lower degree of coalification belonging to low-rank coal; the highest content of CBM can reach 7.17 m<sup>3</sup>/t, and the methane is mainly composed of biogenic gas supplemented by thermogenic gas; the roof lithology of the coal seam is mainly mudstone and siltstone, with good sealing conditions. Finally, two enrichment modes of coalbed methane in slope zones are proposed, namely, the CBM enrichment in the slope zone and the CBM enrichment by fault-hydraulic plugging. The results of this study can serve as a guide for the exploration and development of the deep-buried coalbed methane in the low-rank coal areas.

**Keywords:** Santanghu Basin; Middle Jurassic; Xishanyao Formation; deep CBM enrichment regularity; deep CBM enrichment model



**Citation:** Li, X.; Zhou, J.; Jiao, L.; Sun, B.; Huang, Y.; Huang, D.; Zhang, J.; Shao, L. Coalbed Methane Enrichment Regularity and Model in the Xishanyao Formation in the Santanghu Basin, NW China.

*Minerals* **2023**, *13*, 1369. <https://doi.org/10.3390/min13111369>

Academic Editor: Luca Aldega

Received: 13 September 2023

Revised: 12 October 2023

Accepted: 23 October 2023

Published: 26 October 2023



**Copyright:** © 2023 by the authors. Licensee MDPI, Basel, Switzerland. This article is an open access article distributed under the terms and conditions of the Creative Commons Attribution (CC BY) license (<https://creativecommons.org/licenses/by/4.0/>).

## 1. Introduction

The Santanghu Basin is one of the Jurassic basins in Xinjiang, and its coalbed methane (CBM) of low-rank coal has shown certain exploration prospects [1,2]. As a type of clean energy, CBM has been successfully exploited commercially worldwide [3]. China has abundant CBM resources, with geological resources buried at depths of less than 2000 m reaching  $30.5 \times 10^{12}$  m<sup>3</sup> [4], among which the proportion of CBM resources in low-rank coal is about 34% [5]. The vigorous development and utilization of CBM can contribute to China's energy structure transformation [6] and the "dual carbon goal" [7,8]. Great progress has been made on the exploration and development of the CBM in medium–high-rank coals, such as those in Ordos Basin [9–11], Qinshui Basin [12], and Sichuan Basin [13]. The research on the CBM in the low-rank coals still needs to be deepened, especially because the gas enrichment mechanism and reservoir-forming model of CBM in low-rank coal have not been systematically understood [14].

In recent years, the deep-buried CBM in low-rank coal has become a hot exploration field [15]. Previous studies have analyzed, evaluated, and prospected the CBM resources in low-rank coal and exploration and development prospects in China [14,16–18]. Northwest

China, especially Xinjiang, is rich in the Jurassic coal resources, with most of them being of a low rank [3]. The Jurassic coal basins in Xinjiang are characterized by the preservation of many coal seams, large coal seam thickness, and large resource abundance of coal, making these basins a huge potential for the CBM exploration [19,20]. The Santanghu Basin is a typical low-rank coal basin [17,21]. The coal seams of the Xishanyao Formation of the Middle Jurassic have a stable distribution in the Tiaohu and Malang sags of this basin, forming the material foundation for CBM accumulations [22]. The geological resources of the Tuha-Santanghu Basin reach  $10.6 \times 10^{12} \text{ m}^3$  at a depth of more than 2000 m, and recoverable resources reached  $1.55 \times 10^{12} \text{ m}^3$ , accounting for 15% of the national total [6], suggesting that the study area has great prospects for deep-buried coalbed methane exploration. The exploration and development of CBM in the Santanghu Basin can be helpful for understanding the deep-buried CBM issues and CBM development in low-rank coal issues.

There are many studies on CBM in the Santanghu Basin, but they are all limited to certain aspects [1,2,17,19]. This region is beginning to emerge as a hotspot for CBM exploration and development, and there is an urgent need for a comprehensive synthesis of previous work and more in-depth research into the weaknesses of the study. In this study, geological conditions for CBM enrichment have been investigated, which include coal seam thickness, coal seam burial depth, coal maceral compositions, coal quality, and coal rank. In combination with the sedimentary environments, regional structural characteristics, and hydrogeological conditions, the CBM enrichment model in this basin has been established. It is hoped that the results of this study can serve as a reference for the exploration and development of deep-buried CBM in low-rank coal.

### 2. Geologic Settings

The main Mesozoic basins in northwestern China are compressional in origin, and an orogenic belt formed in response to multiple collisions as the Indian plate interacted with the Eurasia plate, which separated them [23–25]. The Tianshan Mountain range is one of these orogenic belts, and it separates the Junggar Basin from the Tarim Basin and was formed by the collision and docking of the Kazakhstan and Tarim plates. Tectonically, the Santanghu Basin is located at the East Tianshan mountain.

The Santanghu Basin is located in the northeastern part of Xinjiang, northwestern China, and it is adjacent to the Turpan-Hami Basin to the south and the Junggar Basin to the west [26]. The basin is distributed in a long strip shape and extends in a northwest–southeast trended direction. The basin has a length of about 500 km, with its central depression having a maximum width of about 20 km, and the total area is approximately  $2.3 \times 10^4 \text{ km}^2$  (Figure 1).

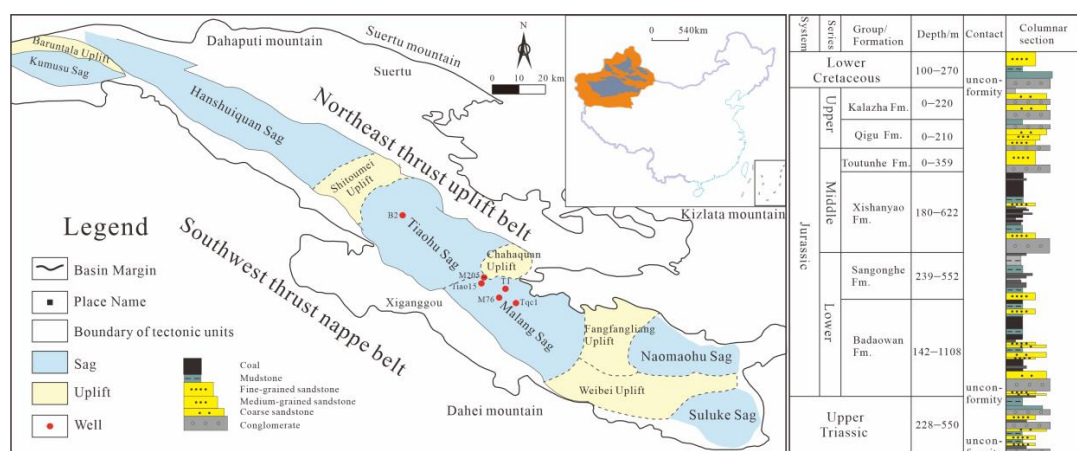


**Figure 1.** Tectonic unit subdivision and columnar section of Santanghu Basin. On the left is the geological outline and tectonic units in the Santanghu Basin with the inset showing location in the Santanghu Basin in China. On the right is the stratigraphic column of the Jurassic in the Santanghu Basin.

The Santanghu Basin is a superimposed and reformed basin on the basement of the Early Paleozoic, and it is distributed between the Altai mountain system and the East Tianshan mountain system. Since the Late Permian, the basin has experienced three development stages, including the foreland basin stage, the extensional depression stage, and the reactivation of foreland basin. The current pattern is an alternation of three primary structural units with uplift and depression from southwest to northeast, namely, the southwest thrust nappe uplift zone, central depression zone, and northeast thrust uplift zone. The central depression zone can be further subdivided into 11 secondary structural units from northwest to southeast, including Kumusu Sag, Baruntala Uplift, Hanshuiquan Sag, Shitoumei Uplift, Tiaohu Sag, Chahaquan Uplift, Malang Sag, Fangfangliang Uplift, Naomaohu Sag, Weibei Uplift, and Suluke Sag [27,28] (Figure 1).

The strata in the Santanghu Basin consist of the Paleozoic, Mesozoic, and Cenozoic. Except for the absence of the Lower Triassic and Upper Cretaceous sedimentary cover layers in the Santanghu Basin, the rest of the strata are relatively well developed, and typically the Carboniferous-Permian and Jurassic strata are relatively thick. The Jurassic coal-bearing series are in angular unconformity contact with the underlying Upper Triassic. The Lower Jurassic features consist of the Badaowan Formation ( $J_{1b}$ ) and Sangonghe Formation ( $J_{1s}$ ) from bottom to top, the Middle Jurassic features consist of the Xishanyao Formation ( $J_{2x}$ ) and Toutunhe Formation ( $J_{2t}$ ) from bottom to top, and the Upper Jurassic features consist of the Qigu Formation ( $J_{3q}$ ) and Kalaza Formation ( $J_{3k}$ ) from bottom to top (Table 1). Among them, the Badaowan Formation and Xishanyao Formation are the main coal-bearing strata, while the Xishanyao Formation is the key target layer for CBM exploration and development due to its larger coal seam thickness.

**Table 1.** Stratigraphic subdivision of the Jurassic in Santanghu Basin.

System	Series	Group/Formation	Contact
Cretaceous	Lower	Tulufan ( $K_{1tg}$ )	unconformity
	Upper	Kalazha ( $J_{3k}$ )	
Jurassic	Middle	Qigu ( $J_{3q}$ )	conformity
		Toutunhe ( $J_{2t}$ )	conformity
	Lower	Xishanyao ( $J_{2x}$ )	conformity
		Sangonghe ( $J_{1s}$ )	conformity
Triassic	Upper	Badaowan ( $J_{1b}$ )	unconformity
		Haojiagou ( $T_{3h}$ )	

### 3. Methods and Data Sources

A total of 17 wells or boreholes were used for their lithological statistics, and contour maps of seam thickness and coal seam depth were drawn (Table S1). A total of 10 coal samples were collected from three wells, including Tangqican 1, Tang 1, and Ma 76 wells, with 3 samples belong to the Tang 1 well, 6 samples belong to the Tangqican 1 well, and 1 sample belong to the Ma 76 well. Sample information can be found in Tables S2 and S3.

The experiments performed in this study included coal macrolithotypes identification, vitrinite reflectance ( $R_o$ , %), coal macerals, and coal proximate analysis. The coal macrolithotypes are classified according to the Chinese National Standard GB/T 18023-2000 [29]. A Leica DM4500P LED microscope was used to determine  $R_o$  and coal macerals following the ICCP (1994) [30–32], respectively. The proximate analysis test was conducted following the Chinese National Standard GB/T 30732–2014 [33].

In addition to the data from collected samples, more data in this paper were from the Research Institute of Exploration and Development, Petro China Tuha Oilfield Company, which are the data we have accumulated over years of experimentation. There are also some data which are from published literature. All data are included in the Supplementary Materials (Tables S1–S5).

## 4. Coal Seam Characteristics and CBM Distribution

### 4.1. Coal Seam Distribution

The coal seams of the Xishanyao Formation are mainly developed in the transitional part between the braided river delta sedimentary system and the lake sedimentary system [34]. The coal seams are developed throughout the area, and the coal accumulation centers are distributed in a NW–SE trended zone, mainly distributed in the northern areas of Tiaohu Sag and Malang Sag. The coal seam thickness in the Tiaohu syncline area can reach over 40 m, while the coal seam thickness in the northern part of Malang Sag can reach 60 m. The coal seam thickness in the southeastern part of Malang Sag is relatively thin, generally 10–20 m. The thickness of coal seams in Naomaohu Sag can reach over 30 m, while the maximum thickness of coal seams in Hanshuiquan Sag can reach over 20 m. In other areas, coal seams are relatively thin, generally less than 10 m (Figure 2).

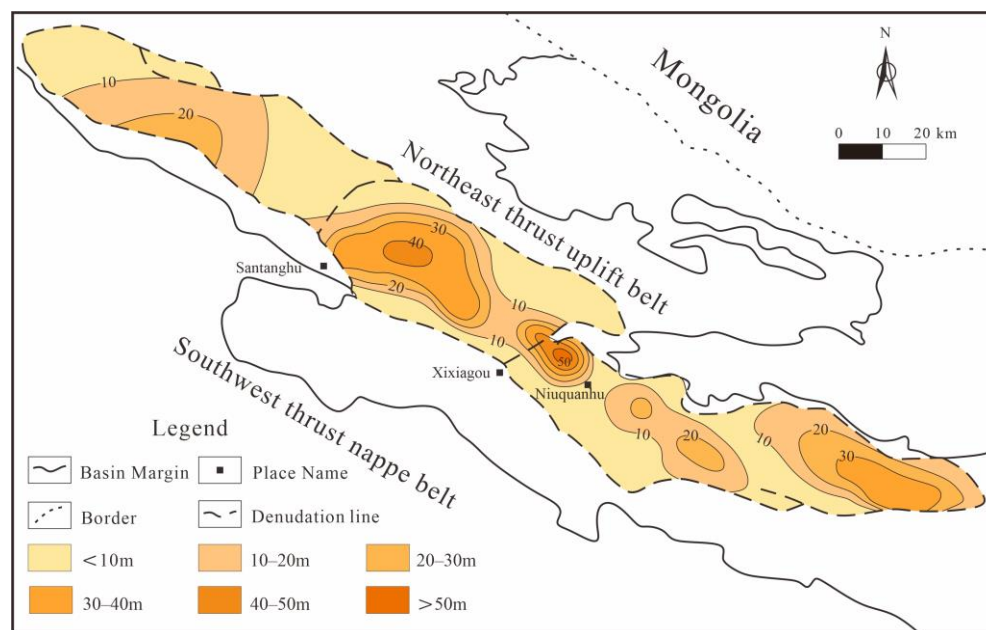


**Figure 2.** Isopach map of coal seam thickness of the Xishanyao Formation in the Santanghu Basin.

The burial depth of the coal seams in the Xishanyao Formation varies greatly, ranging from 500 to 3000 m (Figure 3). Overall, the burial depth of the coal seam in the northern part of the basin is relatively shallow, and gradually increases toward the south. The maximum burial depth is located in the Tiaohu Sag and Malang Sag. The maximum burial depth of the coal seam in the Tiaohu syncline can reach over 2500 m, and the coal seam in the southwest of Malang Sag has the maximum burial depth, being over 2000 m. The coal seams in the Hanshuiquan Sag and Naomaohu Sag are relatively shallow, with burial depths generally less than 1500 m.

### 4.2. Coal Proximate Analysis and Coal Petrology

The coal macrolithotypes are predominantly semi-dull coal, followed by dull coal and semi-dull coal. The original macerals data from the Tang 1 well were not equally spaced in the vertical direction, so three coal samples were added to make them uniformly distributed throughout the coal seam. The maceral compositions are dominated by vitrinite, with the content ranging between 30.0 and 90.0%, averaging 51.4%. The content of inertinite varies from 8.0 to 64.0%, averaging 40.9%. The content of the liptinite is generally low, being less than 10%. The reflectance of vitrinite of coal samples is relatively constant. The vitrinite reflectance ( $R_o$ ) ranges from 0.38 to 0.62%, with most of the values being below 0.5%, indicating a low-rank coal (Tables 2 and S2).

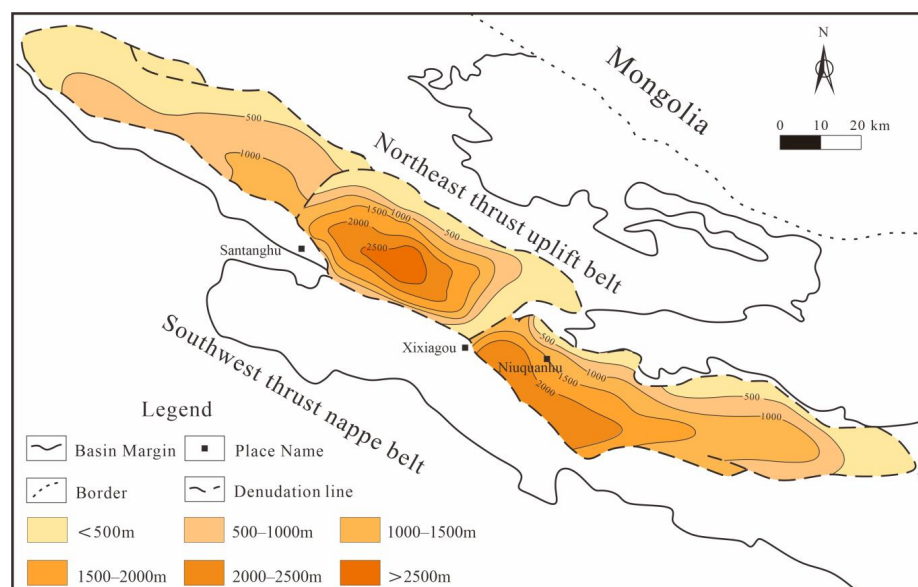


Figure 3. Contours of the coal seam burial depth of the Xishanyao Formation in the Santanghu Basin.

Table 2. Coal macrolithotypes and maceral compositions of the coals in the Xishanyao Formation of Santanghu Basin.

Well ID	Burial Depth (m)	Coal Macrolitho-Type	Maceral Compositions (%)			R <sub>o</sub> (%)
			Vitrinite	Inertinite	Liptinite	
Tangqican1	722.4–757.06	semi-dull	48.7	48.4	2.9	0.61
Tang1	992.31–1027.13	semi-bright	36.1	61.8	2.1	0.45
Tang3	1186.3	semi-dull	90.0	8.0	2.0	0.57
Bei2	1966.2	semi-dull	30.0	64.0	6.0	0.61
Ma205	768.85–768.88	bright	46.0	44.0	10.0	0.38
Ma76	1800.4	semi-bright	60.0	34.0	6.0	0.62
Tiao15	843.72–851.93	semi-dull	44.9	53.8	1.3	0.44

Vitrinite, inertinite, and liptinite content are average of the values given in Table S2; R<sub>o</sub> averaged random vitrinite reflectance under oil-immersed reflected light.

The proximate analysis data from the Tangqican 1 well have significant inconsistencies. To confirm the data’s accuracy, this study has supplemented six more samples at different depths, and the results show that there is still a great difference, indicating that the coal seam here has an obvious heterogeneity. In general, the proximate analysis reveals that the coals of the Xishanyao Formation in the Santanghu Basin have a moisture content ranging from 3.71 to 8.81%, ash yield ranging from 2.58 to 11.94%, and the volatile matter content ranging from 29.47 to 48.22% (Table 3 and S3). Following the China Coal Industry Standards MT/T 849-2000 [35], MT/T 850-2000 [36], and GB/T 15224.1-2018 [37], these coals can be classified as low-to-medium-moisture, high-volatile-matter, and low-ash-yield coals.

Table 3. Results of the partial proximate analysis of the coals in the Xishanyao Formation in the Santanghu Basin.

Well ID	Depth (m)	Proximate Analysis (%)				Data Points
		M <sub>ad</sub>	A <sub>d</sub>	V <sub>daf</sub>	FC <sub>ad</sub>	
Tangqican1	722.29–757.38	8.32	11.92	38.01	50.21	46
Tang1	991.57–1027.13	4.23	2.94	31.42	62.50	11
Tang3	1186.3	6.94	2.58	45.11	49.76	1
Ma205	768.77–768.79	7.73	3.1	46.19	48.12	1
Ma76	1800.4–1806.54	3.00	30.24	21.73	51.80	2
Tiao15	843.72–851.93	8.13	5.28	32.21	59.31	17

M<sub>ad</sub>, moisture on air-dry basis; A<sub>d</sub>, ash yield on dry and ash-free basis; V<sub>daf</sub>, volatile on air-dry basis; and FC<sub>ad</sub>, fixed carbon on air-dry basis.

#### 4.3. Coal Reservoir Characteristics

Coal structure is generally classified into four types, including primary coal, cataclastic coal, granulitic coal, and mylonitic coal [38,39]. The coal structure of the Santanghu Basin is mainly composed of primary coal, followed by cataclastic coal. Primary coal is more conducive to the storage of CBM, but its adsorption capacity and permeability are relatively low compared to cataclastic coal [40]. The permeability of coal seams is mainly influenced by the burial depth and coal body structure [41,42], and as the burial depth increases, the permeability decreases [43,44]. There are significant differences in porosity and permeability of coal seams in different regions and burial depths in Santanghu Basin; the coal sample from the Tang 1 well in the Malang Sag has a permeability of 8.83 mD and porosity of 7.44%. The coal sample from the Tang 2 well in the Tiaohu Sag has a permeability of 0.89 mD and a porosity of 2.25%. The coal sample in Well Tiao 15 in the Malang Sag has a porosity of 9.88%. The coal samples from Naomaohu Sag have a porosity of 6.05%–12.91% with an average of 9.48% [45], and the permeability is 0.69–3.05 mD [41]. The average porosity of the coal in the Hanshuiquan Sag is 11.38%, while the average porosity of the coal in the Naomaohu depression is 9.48%.

#### 4.4. Distribution of the CBM Content

The measured gas content of the Xishanyao Formation coal seam in the Santanghu Basin ranges from 1.71 to 10.00 m<sup>3</sup>/t [46]. The areas with high gas content are located in the Malang and Tiaohu Sags, which can reach over 6 m<sup>3</sup>/t, with the measured gas content in the Tang 1 well reaching the highest of 7.17 m<sup>3</sup>/t (Figure 4). In general, the thicker coal seam would be conducive to the enrichment of CBM [47]. In this study area, there is also a good positive correlation between coal seam thickness and gas content.

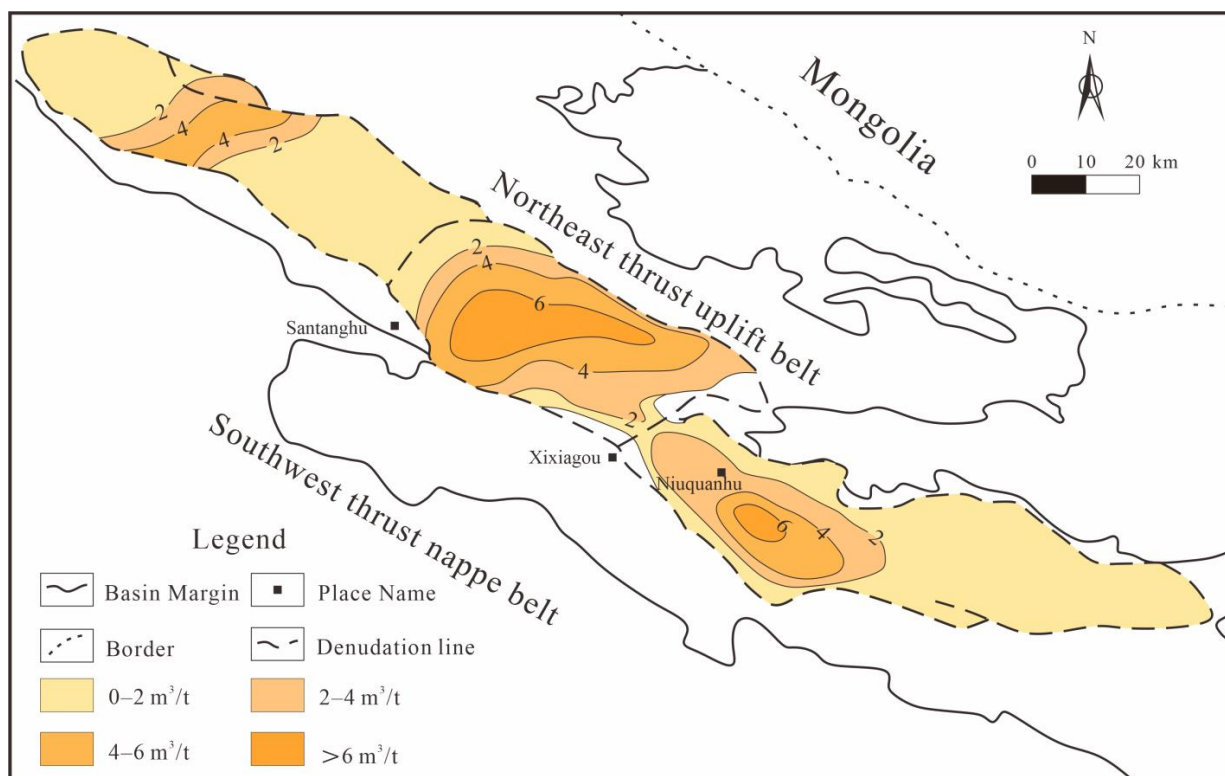


**Figure 4.** Contours of the CBM content of the coals in the Xishanyao Formation in the Santanghu Basin.

## 5. CBM Accumulation

### 5.1. Coal Depositional Conditions

Sedimentary conditions determine the characteristics of coal accumulation, lithofacies assemblage of coal-bearing strata [48,49], spatial distribution of the coal reservoir, and the physical properties of the coal reservoirs and caprocks [50].

The sedimentary environment is closely related to the development of the coal seams, controlling the coal seam thickness, coal quality, and coal physical properties [51,52]. The seams were mainly distributed in the maximum lake flooding surface near the lake transgression system area, and the inter-delta bay, the lake bay of the braided river, and the delta plain area of the downstream braided river would be the most favorable sites for coal accumulation.

Coal seam thickness not only controls the CBM-generating potential of coal reservoirs but also plays an important role in CBM preservation, and the thicker the coal seam, the more favorable it is for CBM preservation [53]. The Xishanyao Formation coal seam in the study area has a thickness of more than 20 m in a single layer, and the coal has mainly a primary structure, which makes for a good CBM reservoir.

The content of inertinite in coal seams is the key parameter controlling the formation of pores and fractures, and the unfilled inertinite has better adsorption capacity [51,54]. In the middle- and low-rank coals, the content of inertinite is positively correlated with the proportion of mesopores and macropores [55]. The macerals of coal seams in different sags in the Santanghu Basin varies greatly, as do the macerals in the same thick coal seam. The content of the inertinite and the vitrinite alternated as the main components (Tables 1 and S2). The vitrinite mainly produces CBM, while the inertinite provides pores for CBM storage, so the layer with a vitrinite/inertinite (V/I) ratio close to 1 can be selected as a favorable layer for CBM development.

### 5.2. Influence of the Sedimentary Successions on CBM Preservation

The low-permeable caprocks will reduce the outward seepage and escape of coalbed methane, and thus play a more important role in CBM reservoir formation than other sedimentary factors [56]. Mudstone has less-developed pores and better sealing ability, making it the best quality caprock, with siltstone being second best [54]. The caprock of the coal seam in the Xishanyao Formation is mainly composed of mudstone and siltstone. The overall sealing performance of the coal seam roof in the basin is good, among which the Malang Sag coal seam roof has the best sealing performance, and the coal seam roof is all thick mudstone (Figure 5).

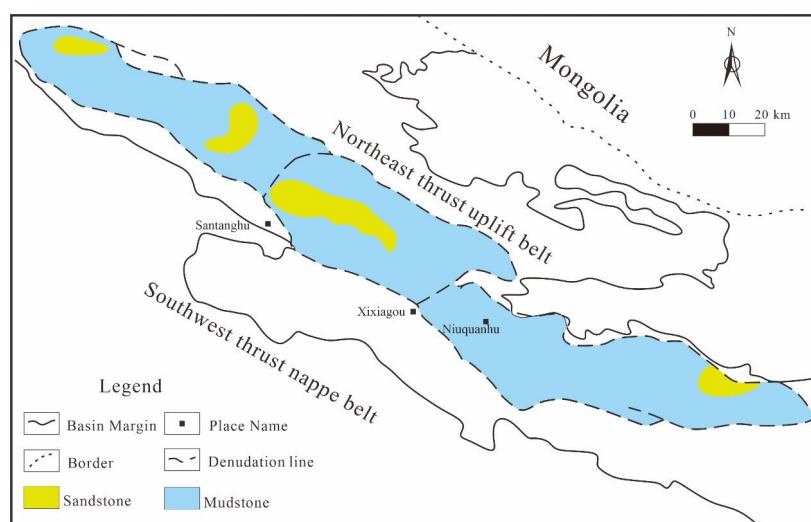


**Figure 5.** Map showing the distribution of the lithologies of the coal roof of the Xishanyao Formation in the Santanghu Basin.

The combination of coals and their roof and floor rocks affects the preservation conditions of CBM and has a direct control effect on CBM [50]. Four lithological associations of the reservoirs and caprocks are identified in the Santanghu Basin, which are characterized by different superimposing combinations of coal and its surrounding rocks (Figure 6). The first combination is represented by the succession of “the fine-grained sandstone –coal–fine-grained sandstone–pebbly sandstone”, which was deposited in a deltaic distributary channel environment (Figure 6a). The second combination is represented by the succession of “the medium-grained sandstone–coal–fine-grained sandstone”, which was deposited in the delta plain environment (Figure 6b). The third combination is represented by the succession of “the siltstone–coal–siltstone”, which was deposited in the coastal and shallow lake environment (Figure 6c). The fourth combination is represented by the succession of “the mudstone–coal–fine-grained sandstone”, which was deposited in the coastal and shallow lake environment (Figure 6d). In consideration of the sealing abilities of different lithological combinations, it can be concluded that the coal seams deposited in coastal and shallow lake environments have a relatively better sealing capacity resulting from the caprock of thick-bedded mudstone and interbedded thin-bedded fine-grained sandstone.

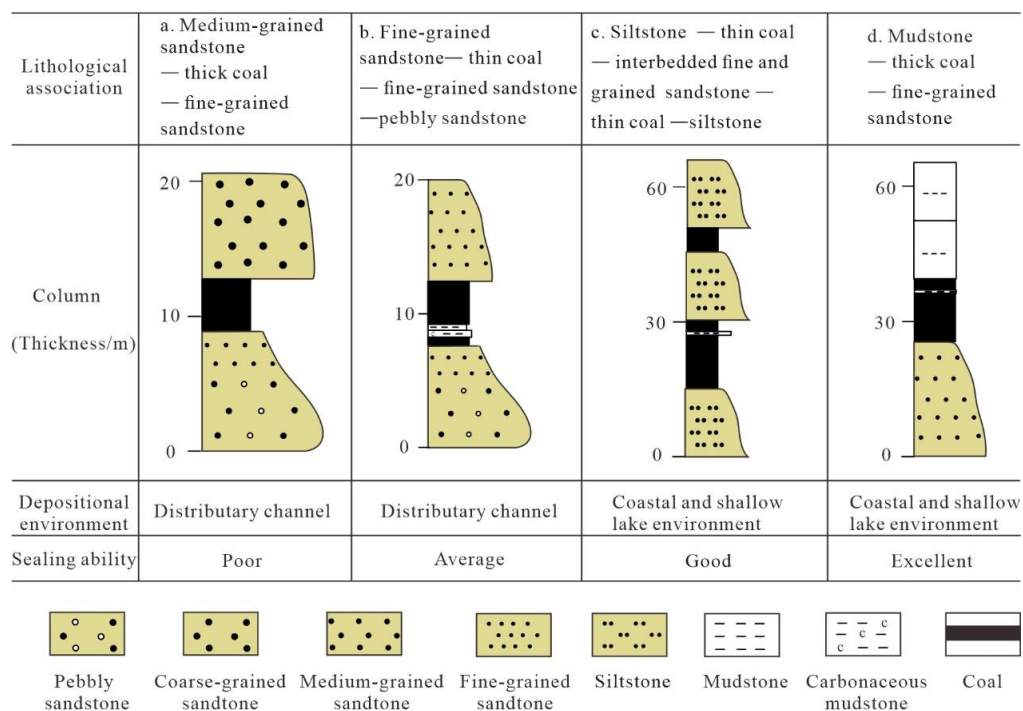


**Figure 6.** CBM preservation ability of different sedimentary successions in the Santanghu Basin. (a,b) show two rock successions from distributary channels, and (c,d) show two rock successions from coastal and shallow lake environments.

5.3. Burial History

The subsidence and uplift of strata caused by tectonic movement will affect the gas generation and storage conditions of coal seams. The Xishanyao Formation in the research area has experienced two distinct subsidence–uplift processes [57]. The first stage of subsidence took place in the Late Jurassic, leading to a coal burial depth of 500–600 m and formation temperature close to 55 °C, and then uplifted to the surface in the Late Jurassic. The second subsidence process took place in the Early Cretaceous, leading to a coal burial depth of nearly 2000 m and formation temperature close to 90 °C. The Early Cretaceous was an important stage for CBM generation in the coals of the Xishanyao Formation in the Tiaohu, Hanshuiquan, and Malang Sags. The coal in the Naomaohu Sag has the lowest degree of coalification and has not reached the threshold of thermal hydrocarbon generation; therefore, there is no generation of thermal gas [45,58]. Simulation experiment of biogenic gas shows that the native methanogen and fermentation bacteria will die in

large numbers when the temperature reaches 55 °C [59]. Therefore, the paleotemperature at that time were not suitable for the survival of methanogen, and there was almost no primary biogenic gas.

#### 5.4. Genetic Analysis of CBM

In general, CBM including biogenic gas and thermogenic gas and these genetic types can be determined by studying the geochemical characteristics of CBM [60–64]. Biogenic CBM can generally be subdivided into primary and secondary biogenic types, with many similarities in their generation mechanisms [64]. The early primary biogenic gas or some thermogenic gas is easy to escape through groundwater flow and the fracture systems [21] and cannot be retained in a large amount in coal seams, while the secondary biogenic gas is widely distributed in coal seams. This study used stable isotopic compositions to analyze the origins of CBM in the Malang and Tiaohu Sags in the Santanghu Basin. The results show  $\delta^{13}\text{C}(\text{CH}_4)$  in the Malang Sag range from  $-64.1\text{‰}$  to  $-54.7\text{‰}$ , and  $\delta\text{D}_{\text{CH}_4}$  range from  $-268\text{‰}$  to  $-239\text{‰}$ . The  $\delta^{13}\text{C}(\text{CH}_4)$  in the Tiaohu Sag range from  $-52.6\text{‰}$  to  $-55.0\text{‰}$ , and  $\delta\text{D}_{\text{CH}_4}$  range from  $-216\text{‰}$  to  $-215\text{‰}$  (Table S4). The cross plots of the  $\delta^{13}\text{C}(\text{CH}_4) - \text{CH}_4/(\text{C}_2\text{H}_6 + \text{C}_3\text{H}_8)$  and the  $\delta\text{D} - \delta^{13}\text{C}(\text{CH}_4)$  indicate that the CBM in the Tiaohu and Malang Sags is dominated by a mixed origin (Figure 7). It can be seen from Figure 7 that the CBM in the coals of the Xishanyao Formation in the Santanghu Basin has a similar origin as the CBM in typical low-rank coal basins such as the Surat Basin.

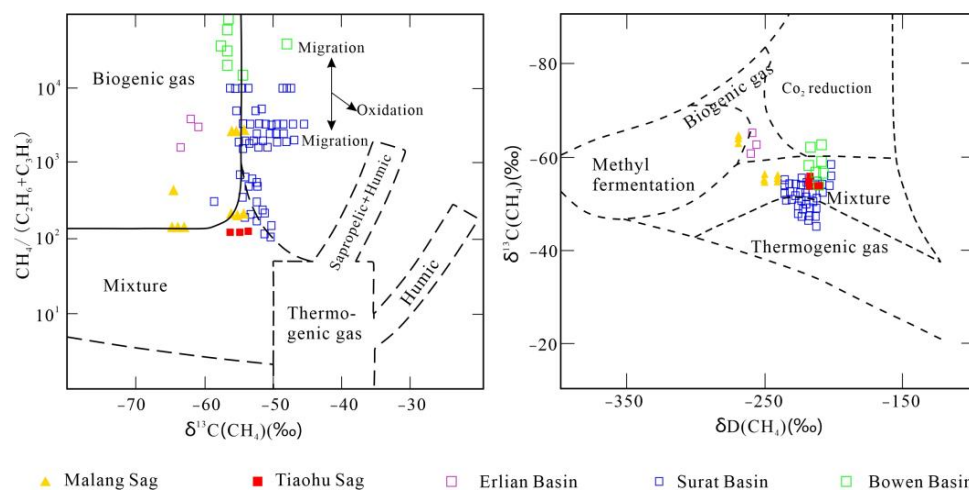


**Figure 7.** CBM genesis identification based on geochemical composition, data from [46]. Also shown are CBM production gases from the Bowen Basin, Queensland [65]; eastern Surat Basin, Australia [66]; Erlian Basin [67].

#### 5.5. Hydrological Factors

CBM is mainly preserved in the pores of coal in an adsorbed state, and hydrogeological conditions have a significant impact on the occurrence and migration of the adsorbed methane, with the latter being crucial for the extraction of CBM [68,69]. The influence of hydrogeological conditions on the CBM preservation in the Santanghu Basin is mainly reflected in two aspects, including the hydraulic migration and the hydraulic plugging. The hydraulic plugging effect is conducive to CBM enrichment.

The favorable area for the enrichment and accumulation of CBM in low-rank coal is the slow groundwater runoff zone, which has a better hydraulic plugging effect on the CBM. The fast runoff in the drainage zones can cause the loss of CBM during transportation, which is very unfavorable for the preservation of CBM [21,46].

The Jurassic strata in the Santanghu Basin belong to a weakly water-rich aquifer, with insufficient surface water replenishment, resulting in the formation of “dry coal seams” [58]. The salinity of coal seam water is high, and the corresponding mineralization is also high (Table 4) [70]. The low mineralization of the coal seam water is suitable for the survival

of methanogen and is conducive to the formation of biogenic gas [71]. The Kumusu, Hanshuiquan, and Naomaohu Sags are the closed weak runoff hydrogeological units, while the Tiaohu and Malang Sags are open local retention hydrogeological units. The open local retention hydrogeological units have a drainage capacity lower than the closed weak runoff units and are conducive to CBM accumulation. When the mineralization of the underground water is higher than 10,000 mg/L, it will cause a large number of deaths of methanogens and also reduce the adsorption capacity of low-rank coal. The mineralization of the coal seam water in the research area is relatively high, but it is less than 10,000 mg/L, and there will still be certain capacity for the formation of biogenic gas (Figure 7).

**Table 4.** Hydrogeological types of Santanghu Basin (also see Table S5 for details).

Structural Units	Mineralization (mg/L)	Water Chemical Type	Hydrogeological Type	Data Source
Kumusu Sag	1800–3400	Na-Cl-SO <sub>4</sub>	confined weak runoff	[70]
Hanshuiquan Sag	1400–3100	Na-Cl-SO <sub>4</sub>	confined weak runoff	[70]
Tiaohu Sag	2400–5000	Na-Cl-SO <sub>4</sub>	open local stagnation	[70]
Malang Sag	1000–5000	Na-HCO <sub>3</sub> -SO <sub>4</sub>	open local stagnation	[70]
Naomaohu Sag	1000–3000	Na-Cl-SO <sub>4</sub>	confined weak runoff	[70]
Ma 18	3882	HCO <sub>3</sub> -Na		
Ma 206	5625–5657	Na <sub>2</sub> SO <sub>4</sub>		
Ma 214	3827	NaHCO <sub>3</sub>		
Ma 208	3880	NaHCO <sub>3</sub>		
Ma 209	3155	NaHCO <sub>3</sub>		
Ma 203	1160	Na <sub>2</sub> SO <sub>4</sub>		
Ma 205	4778	NaHCO <sub>3</sub>		
Ma 202	2241	Na <sub>2</sub> SO <sub>4</sub>		
Ma 201	2382	NaHCO <sub>3</sub>		
Xi 9–13	2398	NaHCO <sub>3</sub>		
Xi 9–11	2865	NaHCO <sub>3</sub>		

## 6. CBM Enrichment Models

According to the geological conditions and the characteristics of CBM generation and preservation, we have selected the well sections with gas content to draw cross-sections corresponding to the enrichment models. Two types of CBM enrichment models in the Santanghu Basin are proposed, namely, the CBM enrichment in slope zone and the CBM enrichment by fault-hydraulic plugging.

### 6.1. CBM Enrichment in Slope Zone

The runoff along the northern edge of the Malang and Tiaohu Sags in the central part of the Santanghu Basin are supplied by atmospheric precipitation and melting water from ice and snow. The runoff infiltrates the aquifer through the surface and flows deep into the coal seam, diluting the mineralization of the coal seam water when flowing through the coal seam, and forming low-mineralization groundwater. Therefore, the mineralization of the coal seam water is low, about 1000–5000 mg/L, which is suitable for the reproduction, growth, and survival of methanogens. Groundwater carrying methanogen converts organic matter into methane gas, thus providing favorable conditions for the generation of secondary biogenic gas. The depth of methane weathering zone in the Santanghu Basin is generally between 400 and 1000 m [70], and the depth of the methane weathering zone in the Malang and Tiaohu Sags is generally between 300 and 400 m, with a maximum depth of no more than 600 m. When the strata in the slope zone are affected by tectonic processes, such as changes in syncline or anticline structures, a relatively gentle slope break zone will be formed, which is more conducive to the enrichment of CBM. The  $R_o$  of deep-buried coal seams reaches 0.80% [46], indicating the mixed genetic characteristics of thermal and secondary biogenic gases. The continuous supply of surface water forms a confined water seal, which is beneficial for the preservation of CBM. Therefore, the CBM accumulates and forms in the coals of the slope zones (Figure 8).

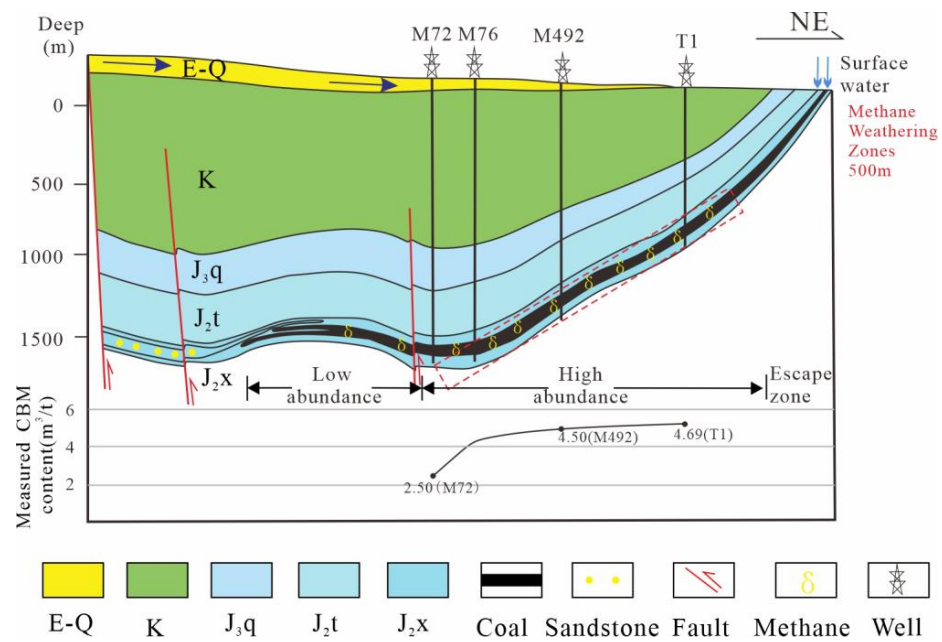


Figure 8. CBM accumulation model in the slope zone of the Santanghu Basin.

6.2. CBM Enrichment by Fault-Hydraulic Plugging

There are many thrust faults in the Malang and Tiaohu Sags. It can be seen from the gas content and structural belt distribution (Figure 9) that the maximum gas content is located in the syncline between two thrust faults. The two thrust faults compress toward the syncline axis, and the atmospheric rainfall supplies the groundwater into the coal seam. The pressure of confined water and the compression pressure of the thrust fault can better seal the CBM and prevent the upward escape of the CBM. In the central depression area of the Tiaohu Sag in the Santanghu Basin,  $\delta^{13}C_{CH_4}$  of the CBM ranges between  $-54.0\text{‰}$  and  $-54.1\text{‰}$ , and  $\delta D_{CH_4}$  is between  $-216\text{‰}$  and  $-215\text{‰}$ , mainly showing an origin of thermogenic gas [46]. The thermal simulation results for low-rank coal show that the amount of thermogenic gas per ton of coal exceeds  $18\text{ m}^3$  [72]. Therefore, the high-abundance CBM reservoirs can also be formed.

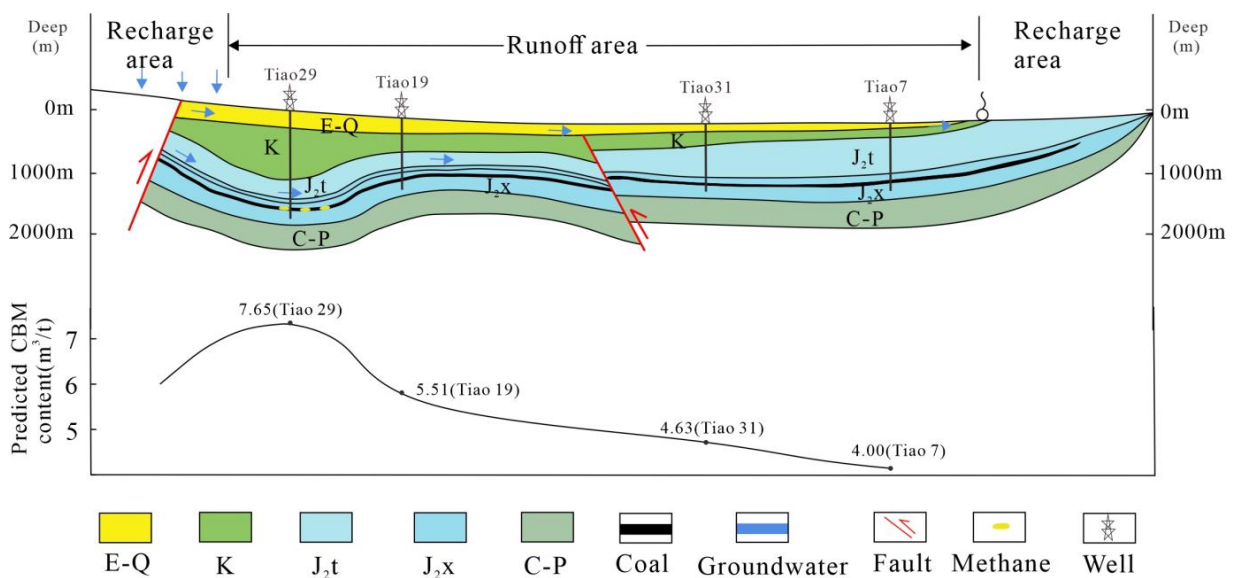


Figure 9. Fault-hydraulic plugging reservoir formation model.

## 7. Conclusions

- (1) The CBM geological conditions in the Santanghu Basin are characterized by a greater total coal seam thickness (10.5–61.3 m) and various coal burial depths (500–2600 m). The coal accumulation center is located in the Tiaohu Sag and Malang Sag, and the deepest burial depth is also located in these two sags. The  $R_o$  is generally 0.38%–0.62%, mainly composed of lignite and long flame coal, and the macerals are mainly composed of vitrinite (30%–90%), with certain amounts of inertinite (8.0%–64%).
- (2) The areas of high CBM content correspond to the regional coal accumulation centers, which are located in the Tiaohu and Malang Sags. These sags are favorable blocks for the CBM exploration in the Santanghu Basin, with a CBM content of up to 7.17 m<sup>3</sup>/t. Stable isotopic analysis shows that the CBM is of mixed origin, mainly thermogenic and secondarily biogenic.
- (3) Combining the depositional environments, structure features, and hydrogeological conditions, two types of CBM enrichment models are summarized, including the CBM enrichment in the slope break zone and the CBM enrichment by fault-hydraulic plugging in the reservoir. It is further delineated that the northern slope zone of the Tiaohu and Malang Sags are the sweet spots for the CBM exploration.

**Supplementary Materials:** The following supporting information can be downloaded at: <https://www.mdpi.com/article/10.3390/min13111369/s1>, Table S1: Statistical data of contour maps of coal seam thickness and burial depth; Table S2: Maceral compositions of the coals in the Xishanyao Formation in the Santanghu Basin; Table S3: Results of the partial proximate analysis of the coals in the Xishanyao Formation in the Santanghu Basin; Table S4: Coalbed Methane Isotope Data; Table S5: Hydrogeological types and mineralization of coal seam water of Santanghu Basin.

**Author Contributions:** Conceptualization, X.L. and J.Z. (Jiamin Zhou); Data curation, J.Z. (Jiamin Zhou) and Y.H.; Formal analysis, Y.H.; Investigation, X.L., J.Z. (Jiamin Zhou), L.J. and D.H.; Methodology, L.S.; Resources, X.L., D.H. and J.Z. (Junlang Zhang); Software, Y.H.; Validation, X.L., B.S., D.H. and J.Z. (Junlang Zhang); Writing—original draft, X.L.; Writing—review and editing, J.Z. (Jiamin Zhou) and L.S. All authors have read and agreed to the published version of the manuscript.

**Funding:** This study is supported by the “14th Five-Year Plan” Forward Looking Basic and Important Science and Technology Project of PetroChina Co., LTD. (2021DJ2306) and the China National Petroleum Corporation Major Science and Technology Project (2019E-2501).

**Data Availability Statement:** Data are available in the Supplementary Materials.

**Conflicts of Interest:** The authors declare no conflict of interest.

## References

1. Huang, W.; Li, X.; Li, L.; Yu, F.; Wang, R.; Chen, X.; Miao, D. Prospect analysis of coalbed methane resources exploration in the Santanghu Basin. *Nat. Gas Geosci.* **2011**, *22*, 733–737.
2. Wang, R. Analysis of coalbed methane exploration potential and evaluation of favorable blocks in Santanghu Basin. *China Pet. Chem. Stand. Qual.* **2014**, *34*, 199.
3. Moore, T.A. Coalbed methane: A review. *Int. J. Coal Geol.* **2012**, *101*, 36–81. [[CrossRef](#)]
4. Zhang, D.; Zhu, J.; Zhao, X.; Gao, Y.; Geng, M.; Chen, G.; Jiao, J.; Liu, S. Dynamic assessment of coalbed methane resources and availability in China. *J. China Coal Soc.* **2018**, *43*, 1598–1604. [[CrossRef](#)]
5. Geng, M.; Chen, H.; Chen, Y.; Zeng, L.; Chen, S.; Jiang, X. Methods and results of the fourth round national CBM resources evaluation. *Coal Sci. Technol.* **2018**, *46*, 64–68. [[CrossRef](#)]
6. Qin, Y.; Shen, J.; Shi, R. Strategic value and choice on construction of large CMG industry in China. *J. China Coal Soc.* **2022**, *47*, 371–387. [[CrossRef](#)]
7. Sang, S.; Wang, R.; Zhou, X.; Huang, H.; Liu, S.; Han, S. Review on carbon neutralization associated with coal geology. *Coal Geol. Explor.* **2021**, *49*, 2.
8. Li, Y.; Pan, S.; Ning, S.; Shao, L.; Jing, Z.; Wang, Z. Coal measure metallogeny: Metallogenic system and implication for resource and environment. *Sci. China (Earth Sci.)* **2022**, *65*, 1211–1228. [[CrossRef](#)]
9. Chen, Y.; Tang, D.; Xu, H.; Li, Y.; Meng, Y. Structural controls on coalbed methane accumulation and high production models in the eastern margin of Ordos Basin, China. *J. Nat. Gas Sci. Eng.* **2015**, *23*, 524–537. [[CrossRef](#)]

10. Shen, J.; Li, K.; Zhang, H.; Shabbiri, K.; Hu, Q.; Zhang, C. The geochemical characteristics, origin, migration and accumulation modes of deep coal-measure gas in the west of Linxing block at the eastern margin of Ordos Basin. *J. Nat. Gas Sci. Eng.* **2021**, *91*, 103965. [[CrossRef](#)]
11. Yong, L.; Yang, J.; Pan, Z.; Meng, S.; Wang, K.; Niu, X. Unconventional Natural Gas Accumulations in Stacked Deposits: A Discussion of Upper Paleozoic Coal-Bearing Strata in the East Margin of the Ordos Basin, China. *Acta Geol. Sin.—Engl. Ed.* **2019**, *93*, 111–129.
12. Hou, Y.; Liu, D.; Zhao, F.; Zhong, L.; Emmanuel, N.N.; Zhang, Q. Geological Characteristics Affecting Coalbed Methane: A Case Study in the Anze Area, Southern Qinshui Basin. *Nat. Resour. Res.* **2022**, *31*, 1425–1442. [[CrossRef](#)]
13. Liang, X.; Shan, C.; Li, Z.; Luo, Y. Exploration innovation practice and effective exploitation key technology of mountain coalbed methane—Taking the Junlian coalbed methane field in southern Sichuan Basin as an example. *Nat. Gas Ind.* **2022**, *42*, 107–129.
14. Wang, B.; Qin, Y.; Shen, J.; Wang, G. Summarization of geological study on low rank coalbed methane in China. *Coal Sci. Technol.* **2017**, *45*, 170–179. [[CrossRef](#)]
15. Li, Y.; Xu, L.; Zhang, S.; Wu, J.; Bi, J.; Meng, S.; Tao, C. Gas bearing system difference in deep coal seams and corresponded development strategy. *J. China Coal Soc.* **2023**, *48*, 900–917. [[CrossRef](#)]
16. Wu, Y.; Wang, G.; Wang, Q. Difficulties and development direction of medium and low-rank coalbed methane industry in Xinjiang region. *China Coalbed Methane* **2023**, *20*, 3–5+20.
17. Li, W.; Tian, W.; Sun, B.; Wang, X.; Zhao, Y. Characteristics of low-stage coalbed methane formation, exploration and development technology. *Nat. Gas Ind.* **2008**, 23–24+29+135.
18. Sun, P.; Wang, B.; Sun, F.; Zheng, G.; Li, G.; Wang, H.; Liu, H.; Deng, Z. Study on the formation mode of low-stage coalbed methane in China. *J. Pet.* **2009**, *30*, 648–653.
19. Wang, T.; Shao, L. *Formation Conditions and Resource Evaluation of Jurassic Coal in Northwest China*; Geological Press: Beijing, China, 2013; pp. 143–148.
20. Xu, F.; Hou, W.; Xiong, X.; Xu, B.; Wu, P.; Wang, H.; Feng, K.; Yun, J.; Li, S.; Zhang, L.; et al. The status and development strategy of coalbed methane industry in China. *Pet. Explor. Dev.* **2023**, *50*, 669–682. [[CrossRef](#)]
21. Huangfu, Y. Characterization of coalbed methane formation in the low coal rank of the Tuha-Santanghu Basin. *Geol. Rev.* **2019**, *65*, 153–154. [[CrossRef](#)]
22. Liang, H.; Li, X.; Chang, Y. CBM enrichment regularity and development potential evaluation in Tiaohu-Malang Sag. *China Coalbed Methane* **2016**, *13*, 13–17.
23. Allégre, C.J.; Courtillot, V.; Tapponnier, P.; Hirn, A.; Mattauer, M.; Coulon, C.; Jaeger, J.J.; Achache, J.; Schärer, U.; Marcoux, J.; et al. Structure and evolution of the Himalaya–Tibet orogenic belt. *Nature* **1984**, *307*, 17–22. [[CrossRef](#)]
24. Hendrix, M.S.; Graham, S.A.; Carroll, A.R.; Sobel, E.R.; Mcknight, C.L.; Schulein, B.J.; Wang, Z. Sedimentary record and climatic implications of recurrent deformation in the Tian Shan: Evidence from Mesozoic strata of the north Tarim, south Junggar, and Turpan basins, northwest China. *GSA Bull.* **1992**, *104*, 53–79. [[CrossRef](#)]
25. Li, D. Hydrocarbon occurrences in the petroliferous basins of western China. *Mar. Pet. Geol.* **1995**, *12*, 26–34. [[CrossRef](#)]
26. Zhao, Z.; Guo, Z.; Zhang, C.; Lu, J. Tectonic evolution and petroleum geological significance of the Santanghu Basin, eastern Xinjiang. *J. Peking Univ. (Nat. Sci. Ed.)* **2003**, *2*, 219–228. [[CrossRef](#)]
27. Zhu, B.; Feng, J.; Hu, B.; Wei, X. Recognition of the basement of the Santanghu Basin. *Xinjiang Pet. Geol.* **1997**, *3*, 197–200+191.
28. Liu, S.; Ma, X.; Zhou, J.; Zhang, J.; Fan, L. Delineation of coal-endowed tectonic units and tectonic features in the Santanghu Basin, Xinjiang. *Geol. Rev.* **2017**, *63*, 271–272. [[CrossRef](#)]
29. Standardization Administration of the People’s Republic of China. *Classification of Macrolithotype for Bituminous Coal: GB/T 18023-2000*; Standards Press of China: Beijing, China, 2000.
30. International Committee for Coal and Organic Petrology (ICCP). The new vitrinite classification (ICCP System 1994). *Fuel* **1998**, *77*, 349–358. [[CrossRef](#)]
31. Pickel, W.; Kus, J.; Flores, D.; Kalaitzidis, S.; Christanis, K.; Cardott, B.J.; Misz-Kennan, M.; Rodrigues, S.; Hentschel, A.; Hamor-Vido, M.; et al. Classification of liptinite—ICCP System 1994. *Int. J. Coal Geol.* **2017**, *169*, 40–61. [[CrossRef](#)]
32. International Committee for Coal and Organic Petrology (ICCP). The new inertinite classification (ICCP System 1994). *Fuel* **2001**, *80*, 459–471. [[CrossRef](#)]
33. Standardization Administration of the People’s Republic of China. *Proximate Analysis of Coal by Instrumental Method: GB/T 30732-2014*; Standards Press of China: Beijing, China, 2014.
34. Wang, T.; Tian, Y.; Shao, L.; Lu, J. Sequence-paleogeography and coal accumulation of the early and middle Jurassic in the Junggar Basin. *J. China Coal Soc.* **2013**, *38*, 114–121. [[CrossRef](#)]
35. Bureau of Coal Industry of the People’s Republic of China. *Classification for Volatile Matter of Coal: MT/T 849-2000*; Standards Press of China: Beijing, China, 2000.
36. Bureau of Coal Industry of the People’s Republic of China. *Classification for Total Moisture in Coal: MT/T 850-2000*; Standards Press of China: Beijing, China, 2000.
37. Standardization Administration of the People’s Republic of China. *Classification for Quality of Coal—Part 1: Ash: GB/T 15224.1-2018*; Standards Press of China: Beijing, China, 2018.
38. Groshong, R.H.; Pashin, J.C.; McIntyre, M.R. Structural controls on fractured coal reservoirs in the southern Appalachian Black Warrior foreland basin. *J. Struct. Geol.* **2009**, *31*, 874–886. [[CrossRef](#)]

39. Hou, Q.; Li, H.; Fan, J.; Ju, Y.; Wang, T.; Li, X.; Wu, Y. Structure and coalbed methane occurrence in tectonically deformed coals. *Sci. China Earth Sci.* **2012**, *55*, 1755–1763. [[CrossRef](#)]
40. Wang, H.; Yao, Y.; Liu, D.; Cai, Y.; Yang, Y.; Zhou, S. Determination of the degree of coal deformation and its effects on gas production in the southern Qinshui Basin, North China. *J. Pet. Sci. Eng.* **2022**, *216*, 110746. [[CrossRef](#)]
41. Cao, Z.; Lin, B.; Liu, T. The impact of depositional environment and tectonic evolution on coalbed methane occurrence in West Henan, China. *Int. J. Min. Sci. Technol.* **2019**, *29*, 297–305. [[CrossRef](#)]
42. Li, H.Y.; Ogawa, Y.; Shimada, S. Mechanism of methane flow through sheared coals and its role on methane recovery. *Fuel* **2003**, *82*, 1271–1279. [[CrossRef](#)]
43. Meng, Z.; Tain, Y.; Li, G. Relationship and control mechanism between permeability and geostress in coal reservoirs in the southern Qinshui Basin. *Prog. Nat. Sci.* **2009**, *19*, 1142–1148.
44. Kang, Y.; Sun, L.; Zhang, B.; Gu, J.; Mao, D. Discussion on classification of coalbed reservoir permeability in China. *J. China Coal Soc.* **2017**, *42*, 186–194. [[CrossRef](#)]
45. Wu, B.; Zhou, L.; Pan, X.; Zhang, Y.; Du, S. Exploration on the genesis of low-stage coalbed methane in the Santanghu Basin, Xinjiang. *Spec. Reserv.* **2020**, *27*, 47–54.
46. Kuang, L.; Wen, S.; Li, S.; Fan, T.; Tian, W.; Wang, X.; Qi, L.; Ying, Y.; Mao, D.; Li, X. Accumulation mechanism and exploration breakthrough of low-rank CBM in the Tuha-Santanghu Basin. *Nat. Gas Ind.* **2022**, *42*, 33–42.
47. Fu, H.; Tang, D.; Xu, T.; Xu, H.; Tao, S.; Zhao, J.; Chen, B.; Yin, Z. Preliminary research on CBM enrichment models of low-rank coal and its geological controls: A case study in the middle of the southern Junggar Basin, NW China. *Mar. Pet. Geol.* **2017**, *83*, 97–110. [[CrossRef](#)]
48. Teichmüller, M. The genesis of coal from the viewpoint of coal petrology. *Int. J. Coal Geol.* **1989**, *12*, 1–87. [[CrossRef](#)]
49. Shao, L.; Wang, X.; Wang, D.; Li, M.; Wang, S.; Li, Y.; Shao, K.; Zhang, C.; Gao, C.; Dong, D.; et al. Sequence stratigraphy, paleogeography, and coal accumulation regularity of major coal-accumulating periods in China. *Int. J. Coal Sci. Technol.* **2020**, *7*, 240–262. [[CrossRef](#)]
50. Shen, Y.; Qin, Y.; Guo, Y.; Ren, H.; Wei, Z.; Xie, G. The Upper Permian Coalbed Methane Bearing System and its Sedimentary Control in Western Guizhou, China. *Geol. J. China Univ.* **2012**, *18*, 427–432. [[CrossRef](#)]
51. Sun, B.; Shao, Y.; Gao, Z.; Li, J.; Sun, B.; Yang, M.; Zhou, J.; Yao, H.; Sun, F.; Shao, L. Coalbed Methane Enrichment Characteristics and Exploration Target Selection in the Zhuozishan Coalfield of the Western Ordos Basin, China. *ACS Omega* **2022**, *7*, 43531–43547. [[CrossRef](#)]
52. Zhao, L.; Qin, Y.; Cai, C.; Xie, Y.; Wang, G.; Huang, B.; Xu, C. Control of coal facies to adsorption-desorption divergence of coals: A case from the Xiqu Drainage Area, Gujiao CBM Block, North China. *Int. J. Coal Geol.* **2017**, *171*, 169–184. [[CrossRef](#)]
53. Scott, S.; Anderson, B.; Crosdale, P.; Dingwall, J.; Leblang, G. Coal petrology and coal seam gas contents of the Walloon Subgroup Surat Basin, Queensland, Australia. *Int. J. Coal Geol.* **2007**, *70*, 209–222. [[CrossRef](#)]
54. Xu, H.; Tang, D. Research progress of control mechanism of coal petrology on CBM production. *Coal Sci. Technol.* **2016**, *44*, 140–145+158. [[CrossRef](#)]
55. Yao, Y.; Liu, D.; Tang, S.; Huang, W. Influence and Control of Coal Petrological Composition on the Development of Microfracture of Coal Reservoir in the Qinshui Basin. *J. China Univ. Min. Technol.* **2010**, *39*, 6–13.
56. Chen, G.; Qin, Y.; Hu, Z.; Li, W. Characteristics of reservoir assemblage of deep CBM-bearing system in Baijiahai dome of Junggar Basin. *J. China Coal Soc.* **2016**, *41*, 80–86. [[CrossRef](#)]
57. Feng, S. Sedimentary Evolution and Coal Accumulation of the Lower and the Middle Jurassic in SanTangHu Basin. Master's Thesis, Xinjiang University, Ürümqi, China, 2015.
58. Li, Z.; Li, X.; Liang, H.; Wang, R. Influence of hydrogeologic conditions on low coal rank coalbed methane in Tuha and Santanghu basins. *Xinjiang Pet. Geol.* **2013**, *34*, 158–161.
59. Liu, H.; Liu, C.; Wang, H.; Yang, Y.; Li, J. Simulation of biogenic coalbed methane formation in low rank coal in Northwest China. *Xinjiang Geol.* **2006**, *02*, 149–152.
60. Qin, Y. Progress and review of research on coalbed methane formation in China. *J. Coll. Geol.* **2012**, *18*, 405–418. [[CrossRef](#)]
61. Rice, C.A.; Flores, R.M.; Stricker, G.D.; Ellis, M.S. Chemical and stable isotopic evidence for water/rock interaction and biogenic origin of coalbed methane, Fort Union Formation, Powder River Basin, Wyoming and Montana USA. *Int. J. Coal Geol.* **2008**, *76*, 76–85. [[CrossRef](#)]
62. Kotarba, M.J.; Rice, D.D. Composition and origin of coalbed gases in the Lower Silesian basin, southwest Poland. *Appl. Geochem.* **2001**, *16*, 895–910. [[CrossRef](#)]
63. Zhang, X.; Tao, M.; Wang, W.; Duan, Y.; Shi, B. Generation of biogenic coalbed methane and its resource significance. *Miner. Rock Geochem. Bull.* **2004**, *23*, 166–171.
64. Song, Y.; Liu, S.; Zhang, Q.; Tao, M.; Zhao, M.; Hong, F. Coalbed methane genesis, occurrence and accumulation in China. *Pet. Sci.* **2012**, *9*, 269–280. [[CrossRef](#)]
65. Kinnon, E.C.P.; Golding, S.D.; Boreham, C.J.; Baublys, K.A.; Esterle, J.S. Stable isotope and water quality analysis of coal bed methane production waters and gases from the Bowen Basin, Australia. *Int. J. Coal Geol.* **2010**, *82*, 219–231. [[CrossRef](#)]
66. Hamilton, S.K.; Golding, S.D.; Baublys, K.A.; Esterle, J.S. Stable isotopic and molecular composition of desorbed coal seam gases from the Walloon Subgroup, eastern Surat Basin, Australia. *Int. J. Coal Geol.* **2014**, *122*, 21–36. [[CrossRef](#)]

67. Tao, J.; Shen, J.; Wang, J.; Li, Y.; Li, C. Genetic Types and Exploration Prospect of Coalbed Methane in Jiergalangtu Depression, Erlian Basin. *Geol. J. China Univ.* **2019**, *25*, 295–301. [[CrossRef](#)]
68. Lamarre, R.A. Hydrodynamic and stratigraphic controls for a large coalbed methane accumulation in Ferron coals of east-central Utah. *Int. J. Coal Geol.* **2003**, *56*, 97–110. [[CrossRef](#)]
69. Scott, A.R. Hydrogeologic factors affecting gas content distribution in coal beds. *Int. J. Coal Geol.* **2002**, *50*, 363–387. [[CrossRef](#)]
70. Wang, Q.; Yang, S.; Wang, G.; Xu, H.; Ren, P.; Dong, W. Delineation of methane weathering zones in the Middle-Lower Jurassic coal beds of the Santanghu Basin. *Xinjiang Pet. Geol.* **2020**, *41*, 261–268.
71. Solano-Acosta, W.; Schimmelmann, A.; Mastalerz, M.; Arango, I. Diagenetic mineralization in Pennsylvanian coals from Indiana, USA:  $^{13}\text{C}/^{12}\text{C}$  and  $^{18}\text{O}/^{16}\text{O}$  implications for cleat origin and coalbed methane generation. *Int. J. Coal Geol.* **2008**, *73*, 219–236. [[CrossRef](#)]
72. Lei, H.; Sun, Q.; Sun, B.; Li, W.; Chen, G.; Tian, W. Conditions and main controlling factors of low-stage coalbed methane formation in Holinhe area, Erlian Basin. *Nat. Gas Ind.* **2010**, *30*, 26–30+123–124.

**Disclaimer/Publisher's Note:** The statements, opinions and data contained in all publications are solely those of the individual author(s) and contributor(s) and not of MDPI and/or the editor(s). MDPI and/or the editor(s) disclaim responsibility for any injury to people or property resulting from any ideas, methods, instructions or products referred to in the content.